S©MR

СИБИРСКИЕ ЭЛЕКТРОННЫЕ
МАТЕМАТИЧЕСКИЕ ИЗВЕСТИЯ
Siberian Electronic Mathematical Reports
http://semr.math.nsc.ru
ISSN 1813-3304

Vol. 21, No. 2, pp. B203–B231 (2024)
https://doi.org/10.33048/semi.2024.21.B11

УДК 519.63; 532.685
MSC 76T99

MODELING THE VARIABILITY OF SEISMIC PROPERTIES OF FROZEN MULTIPHASE MEDIA DEPENDING ON TEMPERATURE

G. RESHETOVA, **E. ROMENSKI**

Dedicated to the memory of Sergey Godunov

Abstract: A three-phase model of a deformable porous medium saturated with a mixture of liquid and gas is presented. The derivation of the model is based on the theory of Hyperbolic Thermodynamically Compatible systems (HTC) applied to a mixture of solid, liquid and gas. The resulting governing equations are hyperbolic and satisfy the laws of thermodynamics (energy conservation and entropy growth). Based on the formulated nonlinear model, governing equations for modeling the propagation of small amplitude seismic waves are obtained. These equations have been used to study the variability of wave fields caused by temperature changes in geological media with porous structures saturated with a mixture of liquid and gas. Numerical examples are presented to illustrate the peculiarities of wave propagation in media of varying porosity and different ratios of liquid and gas fractions. The finite difference scheme on staggered grids has been used for the numerical solution.

Keywords: Poroelasticity, three-phase flow, hyperbolic thermodynamically compatible model, wave propagation.

Reshetova, G., Romenski, E., Modeling the variability of seismic properties of frozen multiphase media depending on temperature.

This work is supported by the Mathematical Center in Akademgorodok under the agreement No. 075-15-2022-281 with the Ministry of Science and Higher Education of the Russian Federation.

Received November, 1 , 2024, Published December, 31, 2024.

1 Introduction

Modeling seismic wave fields in the upper layers of the Earth's surface depending on environmental conditions is an urgent task, in particular for developing Arctic territories. For example, global warming with rising temperatures leads to the thawing of permafrost, increasing the risk of disasters associated with the loss of load-bearing capacity of permafrost layers. Another example is the possible sudden release of methane produced by the decomposition of gas hydrate in sedimentary rocks as temperatures rise.

In this regard, there is a need to monitor possible events in the upper layers of the earth when the temperature changes. One possible tool is to track the variability of seismic wave fields depending on the surrounding conditions. To understand the processes of wave propagation in permafrost formations and gas hydrate accumulations, it is necessary to have a mathematical model that allows us to describe processes when external conditions change, in particular, when temperature varies. As the temperature increases, the structure of permafrost changes, the ice it contains melts, and pores filled with water, which may also contain gas, are formed. Similarly, in gas hydrates, as the temperature increases, their degradation occurs with the formation of pores containing both liquid and gaseous phases. Thus, to simulate wave processes in the specified structures, a model of wave propagation in porous media saturated with a multiphase mixture of liquids and gases is required. This paper deals with the modeling of wave processes in a porous medium, which is considered to be a three-phase mixture consisting of a deformable skeleton saturated with a mixture of liquid and gas.

Currently, the Biot approach [1, 2] is the most widely used to model processes in saturated porous media; see, for example [3, 4] and the references therein. In recent considerations [5], Biot's approach was used for the modeling of three-phase systems where the effects of partial saturation and the presence of different immiscible fluids (e.g. oil and gas) were taken into account. This generalization of Biot's model requires the introduction of a large number of additional material parameters, and it is unclear whether this approach can be applied to more complex environments. In addition, models based on Biot's theory are essentially linear, and it is problematic to use them to describe nonlinear processes with large deformations.

In this paper, an approach based on the Hyperbolic Thermodynamically Compatible (HTC) systems theory [6, 7] is used to describe multiphase porous media. The class of HTC PDE systems includes many well-posed models of continuum mechanics, and in addition the formalism of HTC systems theory can be applied to design new models of complex media; see [8] and references therein. The governing differential equations of HTC models are well-posed, and their solutions satisfy the laws of thermodynamics (energy conservation and entropy growth). The application of the theory to the modeling of porous media can be found in [9]-[11]. This paper is a

continuation of [12], [13] and its purpose is to study the properties of wave fields depending on the changes in temperature.

The paper is structured as follows. In Section 2, the general three-phase model for the deformed porous medium saturated with the mixture of two fluids is formulated. In Section 3, the linear PDE system for small-amplitude wave propagation is derived from the general nonlinear system. Section 4 includes a series of numerical test simulations that demonstrate a significant influence of temperature variations on the properties of the wave fields near the freezing point of the saturating liquid. A numerical scheme obtained by the staggered grid finite difference approach is presented in the Appendix.

2 Master system of HTC governing equation for multiphase compressible flow in deformed porous medium

The general form of the governing equations that describe the flow of a mixture of compressible fluids in a deformable porous medium is based on a generalization of the HTC model of a saturated porous medium presented in [9]. The generalization can be formulated using the HTC model of multiphase compressible fluid flow [14] with an arbitrary number of components. We limit ourselves to considering a saturating fluid consisting of a mixture of two compressible fluids. Thus, we consider a three-phase medium which is a mixture of a deformable solid and two fluids. Each phase is characterized by its volume fraction in the mixture: α_1 and α_2 are the volume fractions of fluids and α_3 is the volume fraction of the deformable solid. Assume that the saturation constraint $\alpha_1 + \alpha_2 + \alpha_3 = 1$ holds, which means that porosity ϕ is defined as $\phi = \alpha_1 + \alpha_2 = 1 - \alpha_3$. The master system for formulating the model, presented below, is written in terms of mixture state variables $\rho = \alpha_1\rho_1+\alpha_2\rho_2+\alpha_3\rho_3$ - mixture density; $c_1 = \alpha_1\rho_1/\rho$, $c_2 = \alpha_2\rho_2/\rho$, $c_3 = \alpha_3\rho_3/\rho$ - phase mass fractions ($c_1+c_2+c_3 = 1$); $v^i = c_1v_1^i+c_2v_2^i+c_3v_3^i$ - mixture velocity; $w_1^i = v_1^i - v_3^i$, $w_2^i = v_2^i - v_3^i$ - fluid velocities relative to solid phase. The deformation of the medium is characterized by the distortion matrix A_{ik} of the entire mixture. The entropy s characterizes the thermal state of the mixture under the assumption of a single entropy approximation, which is applicable for small variations in phase temperatures.

Thus, the complete master system reads as

$$\frac{\partial \rho v^i}{\partial t} + \frac{\partial (\rho v^i v^k + \rho^2 E_\rho \delta_{ik} + w_n^i E_{w_n^k} + \rho A_{ki} E_{A_{kj}})}{\partial x_k} = 0, \tag{1}$$

$$\frac{\partial \rho}{\partial t} + \frac{\partial \rho v^k}{\partial x_k} = 0, \tag{2}$$

$$\frac{\partial A_{ik}}{\partial t} + \frac{\partial A_{im} v^m}{\partial x_k} + v^j \left(\frac{\partial A_{ik}}{\partial x_j} - \frac{\partial A_{ij}}{\partial x_k} \right) = -\Psi_{ik}, \tag{3}$$

$$\frac{\partial \rho c_a}{\partial t} + \frac{\partial (\rho c_a v^k + \rho E_{w_a^k})}{\partial x_k} = 0, \qquad a = 1, 2, \tag{4}$$

$$\frac{\partial w_a^k}{\partial t} + \frac{\partial (w_a^l v^l + E_{c_a})}{\partial x_k} + v^l \left(\frac{\partial w_a^k}{\partial x_l} - \frac{\partial w_a^l}{\partial x_k} \right) = -\Lambda_a^k, \quad a = 1, 2 \tag{5}$$

$$\frac{\partial \rho \alpha_a}{\partial t} + \frac{\partial \rho \alpha_a v^k}{\partial x_k} = -\Phi_a, \quad a = 1, 2, \tag{6}$$

$$\frac{\partial \rho s}{\partial t} + \frac{\partial \rho s v^k}{\partial x_k} = Q. \tag{7}$$

This system consists of the following equations: (1) is the total momentum conservation law for the mixture, (2) is the mass conservation law for the mixture, (3) is the evolution equation for the distortion, (4) is the mass conservation law for fluids (phases 1 and 2), (5) is the equation for the velocities of fluids relative to the solid phase, (6) is the balance equation for the volume fraction of fluids, (7) is the balance law for the entropy of the mixture. Summation over repeated indices $i, j, k, \ldots = 1, 2, 3$ is implied. Summation over repeating phase indices $a, b, c = 1, 2, 3$ is not implied unless otherwise indicated using the summation symbol.

The source terms $-\Psi_{ik}$, $-\Lambda_a^k$, $-\Phi_a$ in equations (3), (5), (6) control the dissipative processes in the mixture and correspond to inelastic deformations, interfacial friction, and phase pressure relaxation to a common value, respectively. The source term Q in the entropy balance law (7) is the entropy production term, which, as we will see below, is nonnegative due to the definition of dissipative terms.

The main closing relation that defines the fluxes and source terms in the system (1) - (7) is the generalized internal energy E, which depends on the state variables $\rho, A_{ik}, c_1, c_2, \alpha_1, \alpha_2, w_1^k, w_2^k, s$. The source terms in (3), (5), (6) are defined via thermodynamic forces - derivatives of E with respect to the state variables E_ρ, $E_{A_{kj}}$, E_{w_k}, E_{c_a}, E_s. The formulas for calculating the source terms are as follows:

$$\Phi_a = \rho \sum_{b=1}^{2} \phi_{ab} E_{\alpha_b}, \quad \Lambda_a^k = \sum_{b=1}^{2} \lambda_{ab} E_{w_b^k}, \quad \Psi_{ik} = \frac{1}{\theta} E_{A_{ik}}, \quad a = 1, 2. \tag{8}$$

Here, Φ_a describes the relaxation of phase pressures to a common value, Λ_a^k simulates the interfacial friction between phases, and Ψ_{ik} is the rate of inelastic deformation of the entire mixture. Relaxation parameters ϕ_{ab}, λ_{ab}, θ may depend on state variables, and ϕ_{ab}, λ_{ab} are assumed to be symmetric with respect to a and b due to Onsager's principle. The source of entropy production Q in the law of entropy balance is expressed as a quadratic form of thermodynamic forces

$$Q = \frac{\rho}{E_s}\left(\sum_{a=1}^{2}\sum_{b=1}^{2}\phi_{ab}E_{\alpha_a}E_{\alpha_b} + \sum_{a=1}^{2}\sum_{b=1}^{2}\lambda_{ab}E_{w_a^k}E_{w_b^k} + \frac{1}{\theta}E_{A_{ik}}E_{A_{ik}}\right) \geq 0. \tag{9}$$

The positive definiteness of the matrices ϕ_{ab}, λ_{ab} and the positivity of θ ensure the positivity of Q, which means that the second law of thermodynamics is satisfied.

The functions describing the thermodynamic state of the medium are calculated using the derivatives of the generalized internal energy, the pressure of the mixture reads as $p = \rho^2 E_\rho$, and the shear stress reads as $\sigma_{ij} = -\rho A_{ki} E_{A_{kj}}$.

The energy conservation equation (first law of thermodynamics) holds for the system (1) - (7) in the form

$$\frac{\partial \rho(E + v^i v^i/2)}{\partial t} + \frac{\partial(\rho v^k(E + v^i v^i/2) + \Pi_k)}{\partial x_k} = 0, \tag{10}$$

where $\Pi_k = v^k p - v^i \sigma_{ik} + \sum\limits_{a=1}^{2} \rho v^l w_a^l E_{w_a^k} + \sum\limits_{a=1}^{2} \rho E_{c_a} E_{w_a^k}$ is the energy flux.

The presented system (1) - (7) can be transformed to a symmetric form using generating variables and generating potential, as is usually done in Symmetric Hyperbolic Thermodynamically Compatible (SHTC) theory [8]. If we assume that this system belongs to the class of SHTC systems, then it requires convexity of the generalized internal energy, although proving convexity is a very difficult task. However, if the energy is not convex and the Hessian matrix consisting of the second derivatives of the energy with respect to the state variables has zero eigenvalues, then the system is still hyperbolic, since the equations have an independent set of eigenvectors and belong to Hyperbolic Thermodynamically Compatible (HTC) class.

In the paper, we consider a three-phase model of a deformable porous medium saturated with a mixture of two fluids, and the closing relations for such a mixture are presented below. As is noted above, the main closing relation for (1) - (7) is the generalized energy E and we define it as a sum of the kinematic energy of the relative motion E_1, the energy of volumetric deformation E_2, and the energy of shear deformation E_3:

$$E = E_1(c_1, c_2, w_1, w_2) + E_2(\alpha_1, \alpha_2, c_1, c_2, \rho, s) + E_3(c_1, c_2, \rho, s, A), \tag{11}$$

where

$$E_1 = \frac{1}{2}\sum_{a=1}^{2} c_a w_a^i w_a^i - \frac{1}{2}(\sum_{a=1}^{2} c_a w_a^i)^2, \tag{12}$$

$$\rho E_2(\alpha_1,\alpha_2,c_1,c_2,\rho,s) = \alpha_1\rho_1 e_1(\rho_1,s) + \alpha_2\rho_2 e_2(\rho_2,s) + \alpha_3\rho_3 e_3(\rho_3,s), \tag{13}$$

$$E_3 = \frac{1}{8}c_{s,M}^2\left(tr(\mathbf{g}^2) - 3\right). \tag{14}$$

The energy of relative motion (12) can be determined in a single way if the kinetic energy of the motion of the mixture is defined as the sum of the kinetic energies of the phases because the following identity takes place

$$\rho\left(\frac{v^i v^i}{2} + E_1\right) = \alpha_1\rho_1\frac{v_1^i v_1^i}{2} + \alpha_2\rho_2\frac{v_2^i v_2^i}{2} + \alpha_3\rho_3\frac{v_3^i v_3^i}{2}. \tag{15}$$

We take the volumetric deformation energy (13) as the mass-averaged energy of the phases $e_a(\rho_a, s)$, $(a = 1, 2, 3)$. For calculation of thermodynamic forces E_ρ, E_{c_a}, E_{α_a} it is convenient to consider an equivalent form of (13)

$$E_2(\alpha_1,\alpha_2,c_1,c_2,\rho,s) = c_1 e_1\left(\frac{\rho c_1}{\alpha_1}, s\right) + c_2 e_2\left(\frac{\rho c_2}{\alpha_2}, s\right) + c_3 e_3\left(\frac{\rho c_3}{\alpha_3}, s\right). \tag{16}$$

The energy E_3 of shear deformation depends on the distortion of the entire mixture through the normalized Finger strain tensor $\mathbf{g}$: $\mathbf{g} = \mathbf{G}/(\det\mathbf{G})^{1/3}$, $\mathbf{G} = \mathbf{A}^T\mathbf{A}$, and $c_{s,M}$ is the squared shear sound velocity of the mixture. The shear sound velocity of the mixture should depend on the phase ratio and is defined by the simple mixture rule

$$c_{s,M}^2 = c_1 c_{s,1}^2 + c_2 c_{s,2}^2 + c_3 c_{s,3}^2, \tag{17}$$

where $c_{s,a}$, $a = 1, 2, 3$ are phase shear sound velocities connected with phase shear moduli μ_a by relation $c_{s,a}^2 = \mu_a/\rho_a$. In our case, we assume that the saturating fluids are inviscid and that their shear moduli are zero $\mu_a = 0, a = 1, 2$. Thus, the mixture shear sound velocity reads as

$$c_{s,M}^2 = c_3 c_{s,3}^2 = (1 - c_1 - c_2)c_{s,3}^2. \tag{18}$$

and the fluids viscosity affects only the interfacial friction coefficients.

Thermodynamic forces E_{α_a}, E_ρ, $E_{A_{kj}}$, $E_{w_a^k}$, E_{c_a}, $p = \rho^2 E_\rho$, $\sigma_{ij} = -\rho A_{ki} E_{A_{kj}}$, $T = E_s$ can be computed with the use of definition of generalized internal energy (11) - (18)

$$E_{\alpha_a} = \tfrac{p_3 - p_a}{\rho}\ (a = 1, 2), \quad p = \rho^2 E_\rho = \alpha_1 p_1 + \alpha_2 p_2 + \alpha_3 p_3,$$

$$\tfrac{\partial E}{\partial \mathbf{A}} = \tfrac{c_{s,M}^2}{2}\mathbf{A}^{-T}\left(\mathbf{g}^2 - \tfrac{tr(\mathbf{g}^2)}{3}\mathbf{I}\right), \quad \sigma_{ij} = -\tfrac{\rho c_{s,M}^2}{2}\left(g_{ik}g_{kj} - \tfrac{1}{3}g_{mn}g_{nm}\delta_{ij}\right),$$

$$E_{w_a^i} = c_a w_a^i - c_a(c_1 w_1^i + c_2 w_2^i) = c_a(v_a^i - v^i), \tag{19}$$

$$E_{c_a} = e_a + \tfrac{p_a}{\rho_a} - e_3 - \tfrac{p_3}{\rho_3} - \tfrac{1}{c_3}E_3 + \tfrac{1}{2}w_a^i(w_a^i - c_1 w_1^i - c_2 w_2^i),\ (a = 1, 2),$$

$$E_s = T = c_1\tfrac{\partial e_1}{\partial s} + c_2\tfrac{\partial e_2}{\partial s} + c_3\tfrac{\partial e_3}{\partial s}.$$

In the next section, when deriving equations for small-amplitude wave fields, we will use the equivalent (1) - (7) system of equations written in terms of phase state variables:

$$\frac{\partial(\alpha_1\rho_1 v_1^i + \alpha_2\rho_2 v_2^i + \alpha_3\rho_3 v_2^i)}{\partial t} +$$

$$\frac{\partial(\alpha_1\rho_1 v_1^i v_1^k + \alpha_2\rho_2 v_2^i v_2^k + \alpha_3\rho_3 v_3^i v_3^k + p\delta_{ik} - \sigma_{ik})}{\partial x_k} = 0, \tag{20a}$$

$$\frac{\partial A_{ik}}{\partial t} + \frac{\partial A_{ij}v^j}{\partial x_k} + v^j\left(\frac{\partial A_{ik}}{\partial x_j} - \frac{\partial A_{ij}}{\partial x_k}\right) = -\frac{\psi_{ik}}{\theta}, \tag{20b}$$

$$\frac{\partial \alpha_1\rho_1}{\partial t} + \frac{\partial \alpha_1\rho_1 v_1^k}{\partial x_k} = 0, \tag{20c}$$

$$\frac{\partial \alpha_2\rho_2}{\partial t} + \frac{\partial \alpha_2\rho_2 v_2^k}{\partial x_k} = 0, \tag{20d}$$

$$\frac{\partial \alpha_3\rho_3}{\partial t} + \frac{\partial \alpha_3\rho_3 v_3^k}{\partial x_k} = 0, \tag{20e}$$

$$\frac{\partial w_1^k}{\partial t} + \frac{\partial\left((v_1^j v_1^j - v_3^j v_3^j)/2 + e_1 + p_1/\rho_1 - e_3 - p_3/\rho_3 + E_3/c_3\right)}{\partial x_k} +$$

$$v^l\left(\frac{\partial w_1^k}{\partial x_l} - \frac{\partial w_1^l}{\partial x_k}\right) = -\Lambda_1^k, \tag{20f}$$

$$\frac{\partial w_2^k}{\partial t} + \frac{\partial\left((v_2^j v_2^j - v_3^j v_3^j)/2 + e_2 + p_2/\rho_2 - e_3 - p_3/\rho_3 + E_3/c_3\right)}{\partial x_k} +$$

$$v^l\left(\frac{\partial w_2^k}{\partial x_l} - \frac{\partial w_2^l}{\partial x_k}\right) = -\Lambda_2^k, \tag{20g}$$

$$\frac{\partial \rho\alpha_1}{\partial t} + \frac{\partial \rho\alpha_1 v^k}{\partial x_k} = -\Phi_1, \tag{20h}$$

$$\frac{\partial \rho\alpha_2}{\partial t} + \frac{\partial \rho\alpha_1 v^k}{\partial x_k} = -\Phi_2, \tag{20i}$$

$$\frac{\partial \rho s}{\partial t} + \frac{\partial \rho s v^k}{\partial x_k} =$$

$$\frac{\rho}{T}\left(\sum_{a=1}^{2}\sum_{b=1}^{2}\phi_{ab}E_{\alpha_a}E_{\alpha_b} + \sum_{a=1}^{2}\sum_{b=1}^{2}\lambda_{ab}E_{w_a^k}E_{w_b^k} + \frac{1}{\theta}E_{A_{ik}}E_{A_{ik}}\right) \geq 0. \tag{20j}$$

3 Governing equations for wave propagation in the porous medium saturated by two-fluid mixture

Our main goal is to study the propagation of small-amplitude waves in a stationary medium, and in this section we derive equations to describe wave processes. The derivation method is based on a standard linearization procedure similar to that described in [9] for a simpler model of an elastic porous medium saturated with a single fluid.

We are particularly interested in studying the variability of wave fields with changes in temperature near the freezing point of the saturating liquid. The rheological properties of a porous medium near the freezing points of the saturating liquid can vary greatly even with small changes in temperature. An initially "frozen" medium such as permafrost or gas hydrate becomes porous as the temperature increases, and the pores are filled with liquid. With an increase in temperature, the size of the pores increases and the liquid can release gas. This is why we are considering a three-phase medium, a mixture of solid, liquid, and gas phases. It is obvious that the material parameters of the medium, namely, density, speed of sound, etc., depend on temperature. We want to obtain equations for wave fields that are applicable at different temperatures, so we will assume that the linearization is performed for a medium in equilibrium at a fixed temperature, which can have different values. Since the range of temperature variations near the freezing point of a liquid under consideration is only a few degrees, we neglect the change in density and sound speed with temperature variation and consider them constant. Porosity can increase significantly from 0 as the saturating liquid melts, so we study the dependence of wave fields only on temperature changes in porosity and material parameters that depend significantly on it.

Thus, let us assume that in a stationary initial motionless state of a medium with a given porosity, the shear stress tensor is zero, the pressure is equal to the external atmospheric pressure, and the temperature corresponds to a constant external temperature and can vary. The given initial state of the medium corresponds to the values of its state variables:

$$\alpha_a = \alpha_a^0, \quad \rho_a = \rho_a^0, \quad v_a^i = 0, \quad s = s_0, \quad A_{ij} = A_{ij}^0, \tag{21}$$

moreover, the constants $\rho_1^0, \rho_2^0, \rho_3^0, s_0$ are determined from the conditions of external equilibrium $p_1(\rho_1^0, s_0) = p_2(\rho_2^0, s_0) = p_3(\rho_3^0, s_0) = p_0$, $T(\rho_1^0, \rho_2^0, s_0) = T_0$, where p_0, T_0 are the external pressure and temperature.

We are interested in temperature variations in the range of several degrees near the freezing point of the saturating liquid. In such a range of temperature changes, the density variations of the three phases are negligibly small (note that the coefficient of volumetric thermal expansions of gas and liquid are of the order of $10^{-3} - 10^{-4} K^{-1}$, and the coefficient of linear expansion of the skeleton material is of the order of $10^{-5} K^{-1}$). Therefore, in order

to simplify the derived equations, we assume that a change in the external temperature does not lead to a change in the phase densities and we will assume that $\rho_1^0, \rho_2^0, \rho_3^0$ are constants independent of temperature and, accordingly, the deformed state of the medium corresponds to the distortion values $A_{ij}^0 = \delta_{ij}$ for an unstressed state of the medium. We can also assume, due to the smallness of the change in initial density with temperature variations, that the initial temperature corresponds to the initial entropy $s_0 = 0$.

The solution to the system (1) - (7) can be found as a small perturbation of the initial state:

$$\alpha_k = \alpha_k^0 + \Delta\alpha_k, \rho_k = \rho_k^0 + \Delta\rho_k, v_k^i = \Delta v_k^i, s = s_0 + \Delta s, A_{ij} = \delta_{ij} + \Delta A_{ij}. \quad (22)$$

Note that $\Delta\alpha_1 + \Delta\alpha_2 + \Delta\alpha_3 = 0$, since $\alpha_1 + \alpha_2 + \alpha_3 = 1$ and $\alpha_1^0 + \alpha_2^0 + \alpha_3^0 = 1$.

Substituting this perturbation into (1) - (7) and discarding perturbations of the solution of order Δ^2 and higher, we obtain the following system

$$\frac{\partial(\alpha_1^0\rho_1^0\Delta v_1^i + \alpha_2^0\rho_2^0\Delta v_2^i + \alpha_3^0\rho_3^0\Delta v_3^i)}{\partial t} + \frac{\partial(\Delta p\delta_{ik} - \Delta\sigma_{ik})}{\partial x_k} = 0, \quad (23a)$$

$$\frac{\partial\Delta A_{ik}}{\partial t} + \frac{\partial\Delta v^j}{\partial x_k} = -\frac{\Delta E_{A_{ik}}}{\theta}, \quad (23b)$$

$$\frac{\partial(\alpha_1^0\Delta\rho_1 + \rho_1^0\Delta\alpha_1)}{\partial t} + \frac{\partial(\alpha_1^0\rho_1^0\Delta v_1^k)}{\partial x_k} = 0, \quad (23c)$$

$$\frac{\partial(\alpha_2^0\Delta\rho_2 + \rho_2^0\Delta\alpha_2)}{\partial t} + \frac{\partial(\alpha_2^0\rho_2^0\Delta v_2^k)}{\partial x_k} = 0, \quad (23d)$$

$$\frac{\partial(\alpha_3^0\Delta\rho_3 + \rho_3^0\Delta\alpha_3)}{\partial t} + \frac{\partial(\alpha_3^0\rho_3^0\Delta v_3^k)}{\partial x_k} = 0, \quad (23e)$$

$$\frac{\partial(\Delta v_1^k - \Delta v_3^k)}{\partial t} + \frac{\partial\left(\Delta p_1/\rho_1^0 - \Delta p_3/\rho_3^0\right)}{\partial x_k} = -\Delta\Lambda_1^k, \quad (23f)$$

$$\frac{\partial(\Delta v_2^k - \Delta v_3^k)}{\partial t} + \frac{\partial\left(\Delta p_2/\rho_2^0 - \Delta p_3/\rho_3^0\right)}{\partial x_k} = -\Delta\Lambda_2^k, \quad (23g)$$

$$\frac{\partial\Delta\alpha_1}{\partial t} = -\Delta\Phi_1, \quad (23h)$$

$$\frac{\partial\Delta\alpha_2}{\partial t} = -\Delta\Phi_1, \quad (23i)$$

$$\frac{\partial\Delta s}{\partial t} = 0. \quad (23j)$$

Here$\Delta p = \Delta(\alpha_1 p_1 + \alpha_2 p_2 + \alpha_3 p_3)$, $\Delta\sigma_{ij} = -\Delta\left(c_3 \frac{\rho c_{s,3}^2}{2}\left(g_{ik}g_{kj} - \frac{1}{3}g_{lk}g_{kl}\delta_{ij}\right)\right)$, $\Delta\Lambda_a^k = \Delta\left(\sum_{b=1}^2 \lambda_{ab} E_{w_b^k}\right)$, $\Delta E_{\mathbf{A}} = \Delta\left(c_3 \frac{c_{s,3}^2}{2}\mathbf{A}^{-T}\left(\mathbf{g}^2 - \frac{tr(\mathbf{g}^2)}{3}\mathbf{I}\right)\right)$, $\Delta\Phi_a = \Delta\left(\rho\sum_{b=1}^2 \phi_{ab} E_{\alpha_b}\right)$.

It should be noted immediately that from equation (23j) it follows that $\Delta s = 0$ and equation (23j) can be neglected. Let us make a further simplifying assumption about the instantaneous relaxation of the phase pressures to a common value. Since the pressures are equalized due to the propagation of waves and their reflection from the phase boundaries, and the characteristic scale of the pore space is small compared to the scales of seismic waves, this assumption is valid. Instantaneous pressure relaxation means $\Delta p_1 = \Delta p_2 = \Delta p_3$, and we obtain for the phase densities perturbations

$$\frac{K_1}{\rho_1^0}\Delta\rho_1 = \frac{K_2}{\rho_2^0}\Delta\rho_2 = \frac{K_3}{\rho_3^0}\Delta\rho_2, \tag{24}$$

where $K_1 = \rho_1^0 \frac{\partial p_1}{\partial \rho_1}|_{\rho_1=\rho_1^0,s=0}$, $K_2 = \rho_2^0 \frac{\partial p_2}{\partial \rho_2}|_{\rho_2=\rho_2^0,s=0}$, $K_3 = \rho_3^0 \frac{\partial p_3}{\partial \rho_3}|_{\rho_3=\rho_3^0,s=0}$ are the phase bulk moduli.

In the complete modified PDE system for wave propagation, two equations (23h), (23i) for perturbations of volume fractions should be replaced by the algebraic equation (24). As a result, to derive PDEs for $\Delta\alpha_1$, $\Delta\alpha_2$, $\Delta\rho_1$, $\Delta\rho_2$ and $\Delta\rho_3$ it is necessary to use the equations (23c) - (23e) and (24).

For interphase friction terms, using (19) and assuming that λ_{ab} is constant, we obtain $\Delta\Lambda_a^k = \sum_{b=1}^2 \lambda_{ab}\Delta E_{w_b^k} = \sum_{b=1}^2 \lambda_{ab}(c_a^0\Delta w_a^i - c_a^0(c_1\Delta w_1^i + c_2\Delta w_2^i))$, where $\Delta w_a^i = \Delta v_a^i - \Delta v_3^i$, $c_a^0 = \alpha_a^0\rho_a^0/\rho^0$, $\rho^0 = \alpha_1^0\rho_1^0 + \alpha_2^0\rho_2^0 + \alpha_3^0\rho_3^0$.

Since we are dealing with small deformations of the medium, we introduce a new state variable $\varepsilon = \frac{1}{2}(\Delta\mathbf{A} + \Delta\mathbf{A}^T)$ - the small strain tensor. For infinitesimal deformations, the Finger strain tensor reads $\mathbf{G} = \mathbf{I} + 2\varepsilon$, and then the normalized Finger tensor can be computed as $\Delta\mathbf{g} = 2(\varepsilon - \frac{1}{3}tr(\varepsilon)\mathbf{I}$. To calculate $\Delta E_{\mathbf{A}}$, one needs to use $\Delta\mathbf{g} = 2(\varepsilon - \frac{1}{3}tr(\varepsilon)\mathbf{I})$ and $\Delta\left(\mathbf{g}^2 - \frac{tr(\mathbf{g}^2)}{3}\mathbf{I}\right) = 2\left(\Delta\mathbf{g} - \frac{1}{3}tr(\Delta\mathbf{g})\mathbf{I}\right)$. Finally, we obtain $\Delta E_{\mathbf{A}} = 2c_3^0 c_{s,3}^2(\varepsilon - \frac{1}{3}tr(\varepsilon)\mathbf{I})$. Similarly, one can compute the perturbation of the stress tensor $\Delta\sigma_{ij} = 2c_3^0 c_{s,3}^2(\varepsilon_{ij} - \frac{1}{3}(\varepsilon_{11} + \varepsilon_{22} + \varepsilon_{33})\delta_{ij})$.

Since we now use the small strain tensor ε_{ij} as a measure of deformation, instead of the distortion equation, we can use the equation for ε_{ij} in the form $\frac{\partial\varepsilon_{ik}}{\partial t} + \frac{1}{2}\left(\frac{\partial\Delta v^j}{\partial x_k} + \frac{\partial\Delta v^k}{\partial x_j}\right) = -\frac{\Delta E_{A_{ik}}}{\theta}$, which can be derived using the definition of ε_{ij} and equation (23b).

We can now write the complete system for wave propagation by introducing the following new notation for the wavefield variables: $V^i = c_1^0\Delta v_1^i + c_2^0\Delta v_2^i + c_3^0\Delta v_3^i$ - total velocity of the three-phase mixture; $W_1^k = \Delta v_1^k - \Delta v_3^k$, $W_2^k = \Delta v_2^k - \Delta v_3^k$ - relative velocities,

$\Sigma_{ik} = 2c_3^0 c_{s,3}^2 \left(\varepsilon_{ij} - \frac{\delta_{ij}}{3}(\varepsilon_{11}+\varepsilon_{22}+\varepsilon_{33})\right)$, - shear stress, $P = \Delta p_1 = K_1\Delta\rho_1 = \Delta p_2 = K_2\Delta\rho_2 = \Delta p_3 = K_3\Delta\rho_3$ - pressure of the mixture.

Using the above notations, we arrive at the following system of linear differential equations:

$$\rho_0\frac{\partial V^i}{\partial t} + \frac{\partial P}{\partial x_i} - \frac{\partial \Sigma_{ik}}{\partial x_k} = \Phi^i, \tag{25a}$$

$$\frac{\partial W_1^i}{\partial t} + \left(\frac{1}{\rho_1^0} - \frac{1}{\rho_3^0}\right)\frac{\partial P}{\partial x_i} = -\Lambda_1^i, \tag{25b}$$

$$\frac{\partial W_2^i}{\partial t} + \left(\frac{1}{\rho_2^0} - \frac{1}{\rho_3^0}\right)\frac{\partial P}{\partial x_i} = -\Lambda_2^i, \tag{25c}$$

$$\frac{\partial P}{\partial t} + K\frac{\partial V^k}{\partial x_k} + K_1'\frac{\partial W_1^k}{\partial x_k} + K_2'\frac{\partial W_2^k}{\partial x_k} = 0, \tag{25d}$$

$$\frac{\partial \Sigma_{ik}}{\partial t} - \mu\left(\left(\frac{\partial V^i}{\partial x_k} + \frac{\partial V^k}{\partial x_i}\right) - \frac{2}{3}\delta_{ik}\left(\frac{\partial V^1}{\partial x_1} + \frac{\partial V^2}{\partial x_2} + \frac{\partial V^3}{\partial x_3}\right)\right) = -\frac{\Sigma_{ik}}{\tau}, \tag{25e}$$

where $c_a^0 = \alpha_a^0\rho_a^0/\rho_0, (a = 1,2)$, $\rho_0 = \alpha_1^0\rho_1^0 + \alpha_2^0\rho_2^0 + \alpha_3^0\rho_3^0$, $K = \left(\frac{\alpha_1^0}{K_1} + \frac{\alpha_2^0}{K_2} + \frac{\alpha_3^0}{K_3}\right)^{-1}$ is the bulk modulus of the mixture and $K_a' = (\alpha_a^0 - c_a^0)K$, $a = 1,2$. Φ^i defines the external force source that excites the wave field.

Interfacial friction terms read as $\Lambda_1^i = \lambda_{11}c_1^0(V_1^i - V^i) + \lambda_{12}c_2^0(V_2^i - V^i)$, $\Lambda_2^i = \lambda_{21}c_1^0(V_1^i - V^i) + \lambda_{22}c_2^0(V_2^i - V^i)$, $V_1^i = \Delta v_1^i, V_2^i = \Delta v_2^i$. Their equivalent form can be written in terms of W_a^i as

$$\Lambda_1^i = \lambda_{11}'W_1^i + \lambda_{12}'W_2^i, \qquad \Lambda_2^i = \lambda_{21}'W_1^i + \lambda_{22}'W_2^i, \tag{26a}$$

$$\begin{pmatrix} \lambda_{11}' & \lambda_{12}' \\ \lambda_{21}' & \lambda_{22}' \end{pmatrix} = \begin{pmatrix} \lambda_{11} & \lambda_{12} \\ \lambda_{21} & \lambda_{22} \end{pmatrix}\begin{pmatrix} (1-c_1^0)c_1^0 & -c_1^0c_2^0 \\ -c_1^0c_2^0 & (1-c_2^0)c_2^0 \end{pmatrix}. \tag{26b}$$

Below we will clarify the choice of λ_{ij} for a solid-liquid-gas mixture.

3.1. Hyperbolicity and energy dissipation. The derived linear system (25) for small amplitude wave propagation in deformed porous medium saturated with a mixture of two fluids is hyperbolic (symmetric hyperbolic in the sense of Friedrichs). The interfacial friction terms in equations (25b), (25c) and the shear stress relaxation term in (25e) are dissipative, which means that they provide wave attenuation and dissipation of the energy.

Symmetric hyperbolicity can be proved by the standard procedure of SHTC theory. To do this, it is necessary to define the generating potential and the generating variables (see, for example, [6], [8]). The energy (11) reduced to the case of small perturbations for the system (25) can be taken

in the form

$$\mathcal{E} = \rho_0 \frac{V_i V_i}{2} + \frac{\rho_0}{2} \sum_{a=1}^{2} c_a^0 W_a^i W_a^i - \frac{\rho_0}{2} (\sum_{a=1}^{2} c_a^0 W_a^i)^2 + \frac{1}{2K} P^2 + \frac{\Sigma_{ij}\Sigma_{ij}}{2\mu}. \quad (27)$$

If we multiply equations (25a) - (25e) by $\mathcal{E}_{V^i} = V^i$, $\mathcal{E}_{W_a^i} = \rho_0(c_a^0 W_a^i - c_a^0(c_1^0 W_1^i + c_2^0 W_2^i))$, $\mathcal{E}_P = P/K$, $\mathcal{E}_{\Sigma_{ik}} = \Sigma_{ik}/\mu$ accordingly and sum all up, then we obtain the energy balance law in the form

$$\frac{\partial \mathcal{E}}{\partial t} + \frac{\partial \Pi_k}{\partial x_k} = -\mathcal{Q}, \quad (28)$$

where $\Pi_k = PV^k + (\alpha_a^0 - c_a^0) P W_a^k - \Sigma_{ik} V^i$ is the energy flux and $\mathcal{Q} = \mathcal{E}_{W_a^i} \Lambda_a^i + \frac{1}{\mu\tau} \Sigma_{ik}\Sigma_{ik}$ is the energy loss.

Following SHTC theory, we introduce the generating variables as listed factors to obtain the law of energy conservation:

$$(q_1, q_2, ..., q_{19}) = (\mathcal{E}_{V^i}, \mathcal{E}_{W_1^i}, \mathcal{E}_{W_2^i}, \mathcal{E}_P, \mathcal{E}_{\Sigma_{ik}}). \quad (29)$$

Then with the use of conservative variables

$$(L_{q_1}, L_{q_2}, ..., L_{q_{16}}) = (\rho_0 V^i, W_1^i, W_2^i, P, \Sigma_{ik}) \quad (30)$$

the generating potential $L = q_i L_{q_i} - \mathcal{E} = \mathcal{E}$ can be calculated.

In terms of generating variables and potential, the system (25) can be written in the Godunov form

$$\frac{\partial L_{q_i}}{\partial t} + \frac{\partial M_{q_i}^k}{\partial x_k} = S_i, \quad (31)$$

where the potentials M^k that generate the fluxes can be calculated similarly to L: $M^k = q_i M_{q_i}^k - \Pi_k = \Pi_k$. S_i are the source terms corresponding to the equations in (25).

It is clear that the system (31) can be written in the equivalent quasilinear form

$$L_{q_i q_j} \frac{\partial q_j}{\partial t} + M_{q_i q_j}^k \frac{\partial q_j}{\partial x_k} = S_i, \quad (32)$$

with symmetric Hessian matrices at the derivatives. If the matrix $L_{q_i q_j}$ is positive definite, then (32) is a symmetric hyperbolic system in the sense of Friedrichs. The positive definiteness of $L_{q_i q_j}$ is easy to prove since the energy (27) is a convex function.

Although the linear system of partial differential equations (25) is hyperbolic, its eigenvalues cannot be found explicitly. Let us just note that in the presented model, as we will see in numerical section, there are three velocities of sound, corresponding to two longitudinal and one transverse waves.

The energy loss is described by the negative source term $-\mathcal{Q}$ in the energy balance law (28), arising from interfacial friction and shear stress relaxation, taken into account by the sources in (25b), (25c), (25e). These sources produce dissipation, which leads to wave attenuation.

A porous medium saturated with a multiphase fluid has complex rheological properties that affect the attenuation of seismic waves. The rheology

of such a medium depends on its structure, the properties of the skeleton, and saturating fluids, which in turn may depend on external conditions. Important factors leading to the dissipation of seismic energy in a porous deformable medium are interfacial friction and relaxation of shear stresses. For the processes of interest to us, near the freezing point of the saturating liquid, a change in porosity occurs, which affects both the magnitude of interfacial friction and the rate of stress relaxation. The numerical test problems considered below show how a change in porosity affects the properties of seismic waves and their attenuation.

3.2. Interfacial friction and shear relaxation terms. Let us discuss the choice of source terms for interfacial friction and their specific form for a gas-liquid-solid mixture. The terms of the friction source in the equations for the relative velocities read $\Lambda_1^i = \lambda_{11} c_1^0 (V_1^i - V^i) + \lambda_{12} c_2^0 (V_2^i - V^i)$, $\Lambda_2^i = \lambda_{21} c_1^0 (V_1^i - V^i) + \lambda_{22} c_2^0 (V_2^i - V^i)$ and include friction via differences between the phase velocities V_a^i and the velocity of the mixture V^i. Since we do not have information about the influence of the friction force of one fluid on the friction force of the other fluid, we assume $\lambda_{12} = 0, \lambda_{21} = 0$. This assumption gives us

$$\Lambda_1^i = \lambda_{11}(c_1^0(1-c_1^0)W_1^i - c_1^0 c_2^0 W_2^i), \Lambda_2^i = \lambda_{22}(-c_1^0 c_2^0 W_1^i + c_2^0(1-c_2^0)W_2^i). \quad (33)$$

Friction coefficients must be determined for each specific case, which requires both theoretical and experimental studies. Therefore, we take the coefficients based on empirical assumptions, limiting ourselves only to a qualitative study of wave fields. Let us assign numbers 1, 2 and 3 to the gas, liquid, and solid phases, respectively. In the numerical examples below, we assume that the friction coefficient between the gas and an entire mixture is much lower than between the liquid and the entire mixture, which means that $\lambda_{11} << \lambda_{22}$. Since in the absence of a gas phase ($c_1^0 = 0$) the coefficient λ_{22} models the friction between a liquid and a solid, it can be taken as $\lambda_{22} = \theta_2^{-1}$ with θ_2 from [9]. Note that in [9] friction force is determined by a comparison with Biot's model. In the same way, for convenience, we denote $\lambda_{11} = \theta_1^{-1}$ and use these parameters in the numerical simulations (see Tables 1 and 2).

As for the shear stress relaxation time, there are no data for porous media that could be used to determine its value and its dependence on state variables. It is intuitively clear that for a porous medium with the same skeleton material, with increasing porosity the material becomes "softer" and the relaxation time should decrease.

Therefore, in the following, using numerical examples, we simply study the properties of wave fields at different gas-to-liquid ratios and different relaxation times. Of course, to solve practical problems, research is required, both theoretical and experimental, to determine the material parameters of porous media, including relaxation times and interfacial friction coefficients.

Table 1. Physical parameters used for simulation in homogeneous test cases.

State	Property	Parameters	Value	Unit
Fluid1:				
(air)	Fluid density	ρ_1^0	1.225	kg/m^3
	Sound velocity	c_1	330	m/s
	Bulk modulus	$K_1 = \rho_1^0 c_1^2$	0.00013	GPa
Fluid2:				
(water)	Fluid density	ρ_2^0	1040	kg/m^3
	Sound velocity	c_2	1500	m/s
	Bulk modulus	$K_2 = \rho_2^0 c_2^2$	2.34	GPa
Solid phase:	Solid density	ρ_3^0	2500	kg/m^3
	P-wave velocity	v_p	6155	m/s
	S-wave velocity	v_s	3787	m/s
	Bulk velocity	c_s	4332	m/s
	Bulk modulus	$K_3 = \rho_3^0 c_s^2$	46.91	GPa
	Shear modulus	$\mu = \rho_3^0 v_s^2$	35.85	GPa
Dissipative parameters:	Interphase friction	θ_1	$3.36 \cdot 10^{-12}$	s
	Interphase friction	θ_2	$3.36 \cdot 10^{-7}$	s
	Relaxation time	τ	10^{-6}	s

4 Numerical simulations

In this section, we numerically analyze the main features of small-amplitude wave propagation in a porous medium associated with the presence of a saturated compressible mixture of two fluids. For the numerical modeling of the system (25), we use finite difference methods of a staggered grid [15]-[17], which are well suited to solve symmetric hyperbolic first-order PDE systems in the velocity-stress formulation. We have developed and implemented an accurate fourth-order scheme in spatial variables and second-order in time for the simulation of wave propagation in a porous medium. The details of this scheme are given in the Appendix.

Test 1. We start the verification of the (25) model by considering a two-dimensional homogeneous poroelastic medium saturated with a mixture of water and gas in a solid deformable skeleton. The properties of the skeleton and pore fluids are given in Table 1.

Simulations were performed for a computational model of $2200 * 2200$ grid nodes with a uniform spatial grid cell of $2.5 \cdot 10^{-5}$ m and a time step of $3.3 \cdot 10^{-9}$ s. The volumetric type source with a frequency of $f_0 = 1$ MHz was placed in the centre of the computational model. To excite the volumetric

type source, source terms were added to the right hand sides of the shear stress relaxation equations (25e) for both components Σ_{11}, Σ_{22}. A source function was defined as the product of the Dirac delta function in space and the pulse function of Ricker wavelet $f(t)$ in time:

$$f(t) = (1 - 2\pi^2 f_0^2 (t - t_0)^2) exp[-\pi^2 f_0^2 (t - t_0)^2], \tag{34}$$

where f_0 is the source frequency and t_0 is the time wavelet delay, equal to $t_0 = 1/f_0$ s in our considerations.

Let us analyze the effect of changing the volume of the saturating fluids on the wave field characteristics. If only one phase is assumed in the model (25) (there are no other two phases), the system of equations must describe a purely elastic medium with given seismic velocities. Depending on the chosen phase, it can be pure solid ($\alpha_3^0 = 1$), pure air ($\alpha_1^0 = 1$), or pure water ($\alpha_2^0 = 1$). To verify this, we present the results of the numerical simulations in Fig. 1, where the wave field snapshots of the norm of the total mixture velocity vector $||V||^2$ at time $t = 5 \cdot 10^{-6}$ s are shown for different cases of the phase volume ratio in the poroelastic model. In order to eliminate the influence of the terms of friction between phases and stress relaxation included as right-hand terms in the equation system (25), we first set them to zero.

As expected, the obtained velocities correspond to the longitudinal wave velocity for a pure solid ($v_p = 6155$ m/s) and the sound velocities for pure air ($c_1 = 330$ m/s) and water ($c_2 = 1500$ m/s) given in Table 1. When estimating velocities, we add a Ricker wavelet delay equal to $1 \cdot 10^{-6}$ s.

Note that in the case of a volumetric source, only one compressional wave appears in a pure solid, water or air (Fig. 1a-1c), while in the poroelastic case we observe the appearance of fast and slow (Biot mode) compressional waves (Fig. 1d). The estimated velocities of 3817 m/s for the fast P-wave and 329 m/s for the slow P-wave agree with the velocity dispersion curves obtained using the standard methodology described in [9].

Test 2. Let us now analyze the influence of the phase ratio in the medium on the formation of the wave field. We find it interesting to consider the effect of the presence of air on the velocity of seismic waves. For this purpose, we consider the poroelastic case (solid+air) with different contents of the air phase α_1^0 and vanished relaxation terms $\theta_1 = \theta_2 = 0, \tau = \infty$.

Horizontal slices of the velocity V^2 at $x_2 = 0$ for different α_1^0 are shown in Fig. 2. As can be seen, at $\alpha_1^0 = 0$, the wave velocity corresponds to the velocity of the P wave in an elastic medium. The velocity of the P-wave decreases as soon as even a small amount of air is present, while its amplitude increases. In addition, the slow Biot P-wave appears. To clarify the details, we show in Fig. 3 the zoomed fragment of Fig. 2. Note that the amplitude of the Bio wave is inversely proportional to the value of alpha.

Test 3. Let us now analyze the influence of interfacial friction on the generation of the wave field. To do this, compare the horizontal wave field slices

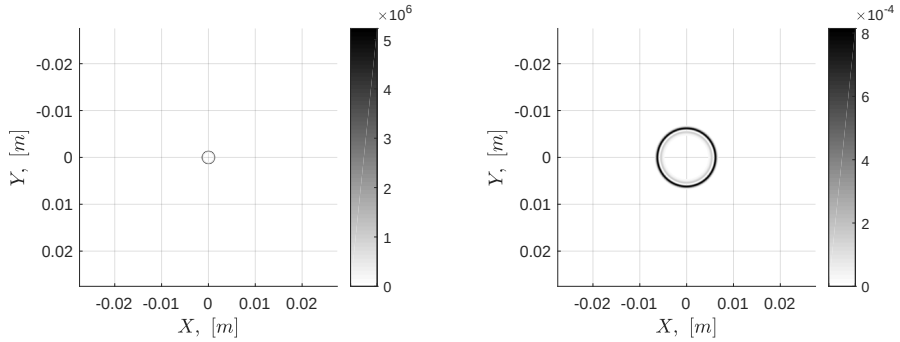

(a) Pure Fluid1 (air): $\alpha_1^0 = 1, \alpha_2^0 = 0, \alpha_3^0 = 0$

(b) Pure Fluid2 (water): $\alpha_1^0 = 0, \alpha_2^0 = 1, \alpha_3^0 = 0$

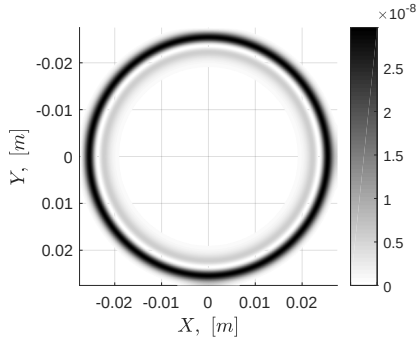

(c) Pure Solid (solid phase): $\alpha_1^0 = 0, \alpha_2^0 = 0, \alpha_3^0 = 1$

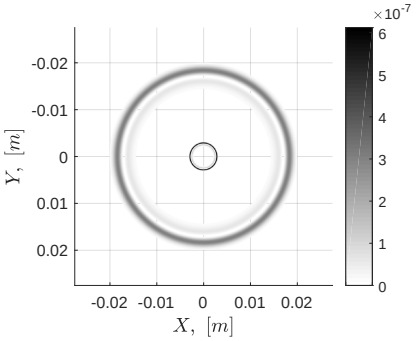

(d) Poroelastic case (solid+water): $\alpha_1^0 = 0, \alpha_2^0 = 0.3, \alpha_3^0 = 0.7$

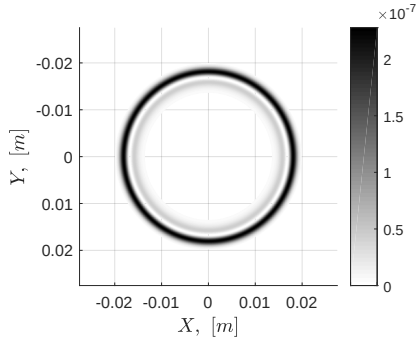

(e) Poroelastic case (solid+air): $\alpha_1^0 = 0.001, \alpha_2^0 = 0, \alpha_3^0 = 0.999$

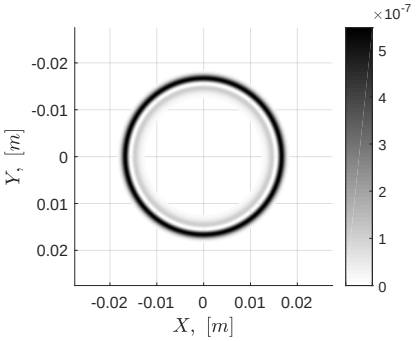

(f) Poroelastic case (solid+water+air): $\alpha_1^0 = 0.001, \alpha_2^0 = 0.3, \alpha_3^0 = 0.699$

Figure 1. Snapshots of the wave field velocity $||V||^2$ for different media: pure air (a), pure water (b), pure solid (c), porous medium with solid and water (d), porous medium with solid and air (e) and with solid, water and air (f) at time $t = 5 \cdot 10^{-6}$ s.

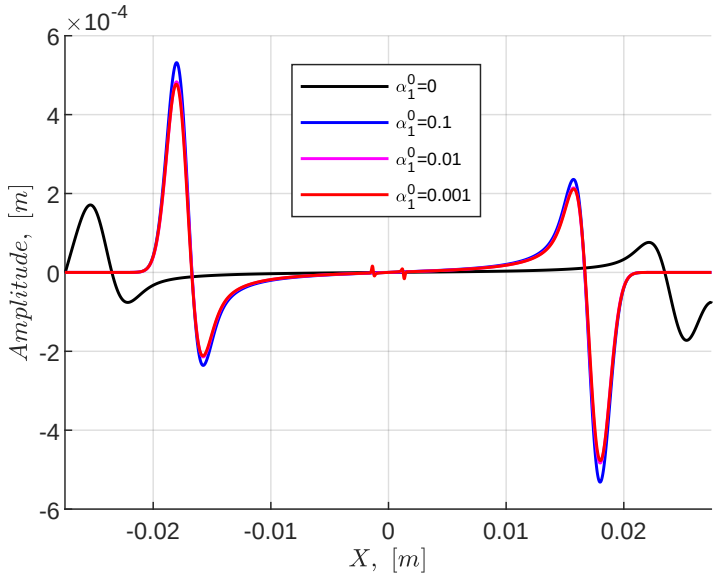

Figure 2. The horizontal slice of V^2 at $x_2 = 0$ for different α_1^0 for the solid-air porous medium with parameters from Table 1 and volume phase fractions $\alpha_1^0 = 0, 0.1, 0.01, 0.001$ and $\alpha_3^0 = 1 - \alpha_1^0$.

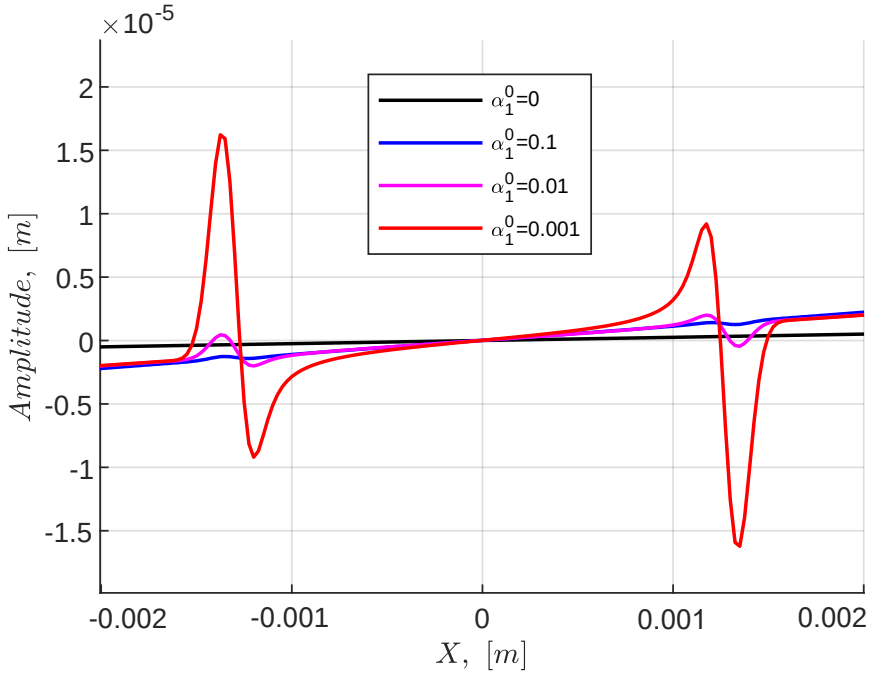

Figure 3. Zoom version of Fig. 2.

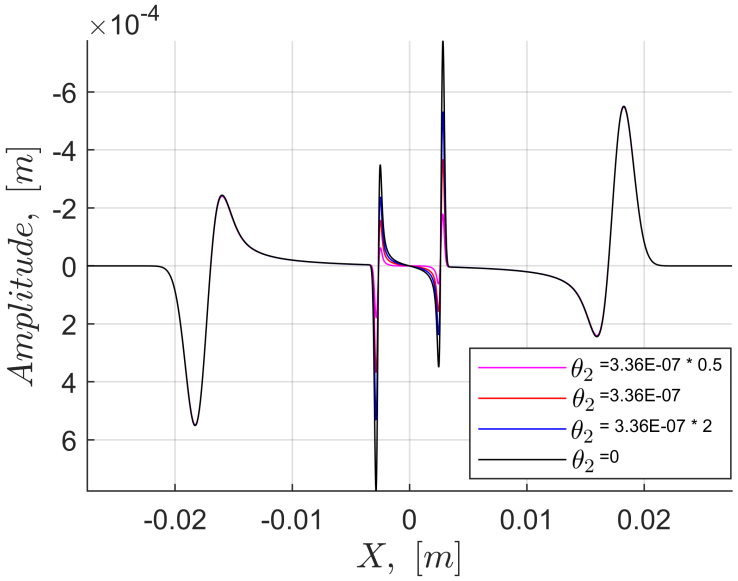

Figure 4. The horizontal slice of V^2 at $x_2 = 0$ for the solid-water porous medium with parameters from Table 1, volume phase fractions $\alpha_2^0 = 0.3, \alpha_3^0 = 0.7$, realxation time $\tau = 5 \cdot 10^{-7}$ and different values of interfacial friction θ_2.

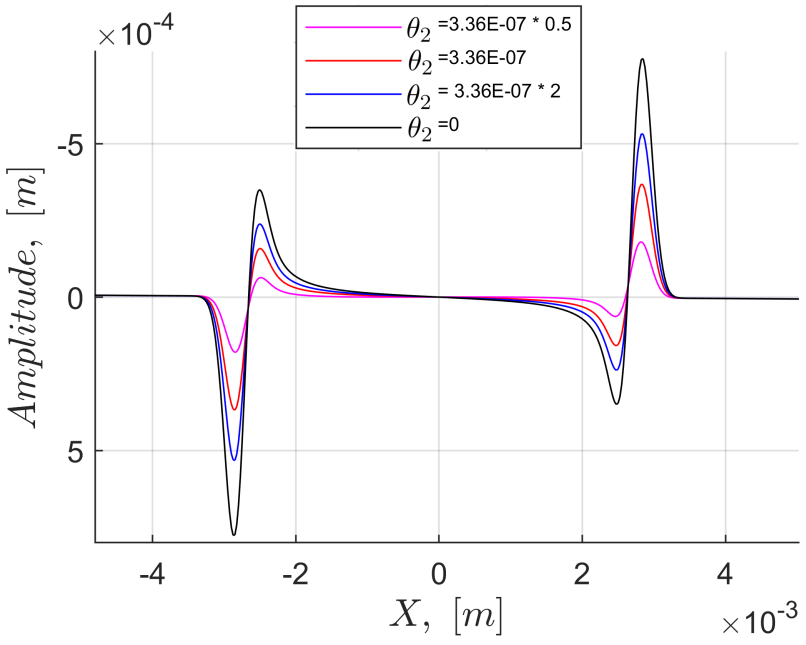

Figure 5. Zoom version of Fig. 4.

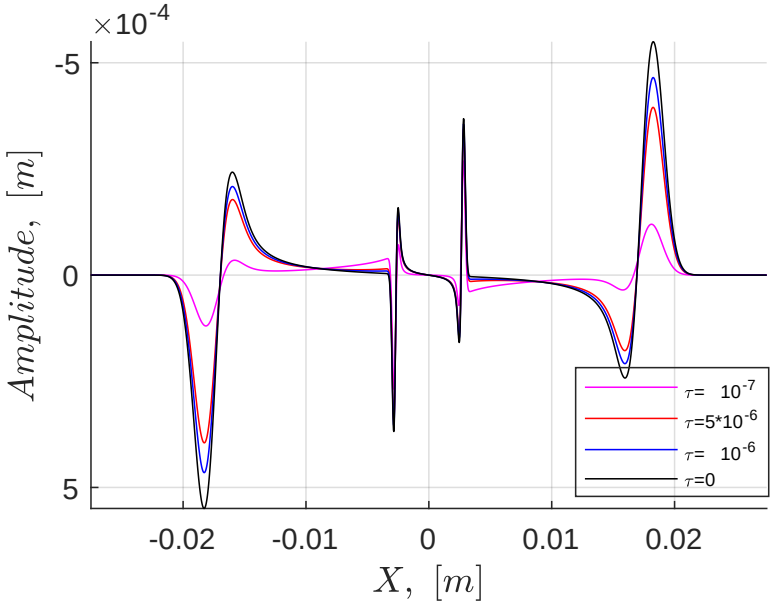

Figure 6. The horizontal slice of V^2 at $x_2 = 0$ for the solid-water porous medium with parameters from Table 1, interphase friction $\theta_2 = 3.36 \cdot 10^{-7}$, $\theta_1 = 3.36 \cdot 10^{-12}$ and different values of realxation time τ.

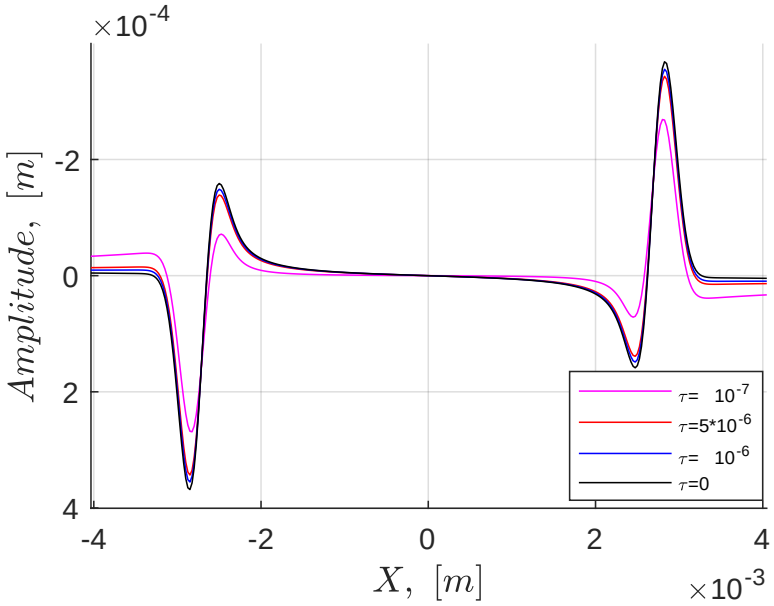

Figure 7. Zoom version of Fig. 7.

Table 2. Physical parameters used for simulation model with Talik Layer.

State	Property	Parameters	Value	Unit
Active layer:				
(solid phase only)	P-wave velocity	v_p	1800	m/s
	S-wave velocity	v_s	900	m/s
	Density	ρ	1500	kg/m^3
Unfrozen layer:				
(solid phase only)	P-wave velocity	v_p	2400	m/s
	S-wave velocity	v_s	1800	m/s
	Density	ρ	2000	kg/m^3
Permafrost layer:				
(solid phase only)	P-wave velocity	v_p	3800	m/s
	S-wave velocity	v_s	2400	m/s
	Density	ρ	2500	kg/m^3
Talik layer:				
(air phase)	P-wave velocity	v_p	330	m/s
	S-wave velocity	v_s	0	m/s
	Density	ρ	1.25	kg/m^3
Talik layer:				
(water phase)	P-wave velocity	v_p	1500	m/s
	S-wave velocity	v_s	0	m/s
	Density	ρ	1040	kg/m^3
Talik layer:				
(solid phase)	P-wave velocity	v_p	3800	m/s
	S-wave velocity	v_s	2400	m/s
	Density	ρ	2500	kg/m^3
Dissipative				
parameters:	Interphase friction	θ_1	$3.36 \cdot 10^{-12}$	s
	Interphase friction	θ_2	$3.36 \cdot 10^{-7}$	s
	Relaxation time	τ	10^{-6}	s

$x_2 = 0$ of the V^2 component simulated for the porous solid+water medium with the parameters from Table 1, volume phase fractions $\alpha_2^0 = 0.3, \alpha_3^0 = 0.7$, relaxation time $\tau = 5 \cdot 10^{-7}$ and different values of interfacial friction θ_2 as shown in Fig. 4. The comparison shows that interfacial friction has almost no effect on the propagation velocity and amplitude of the fast P-wave. However, the slow P-wave responds to this influence by attenuating its amplitude. The velocity of the slow P-wave also does not change significantly. It can be concluded that interfacial friction mainly affects the amplitude of the Biot wave, and the smaller the value of θ_2, the smaller the amplitude of the wave.

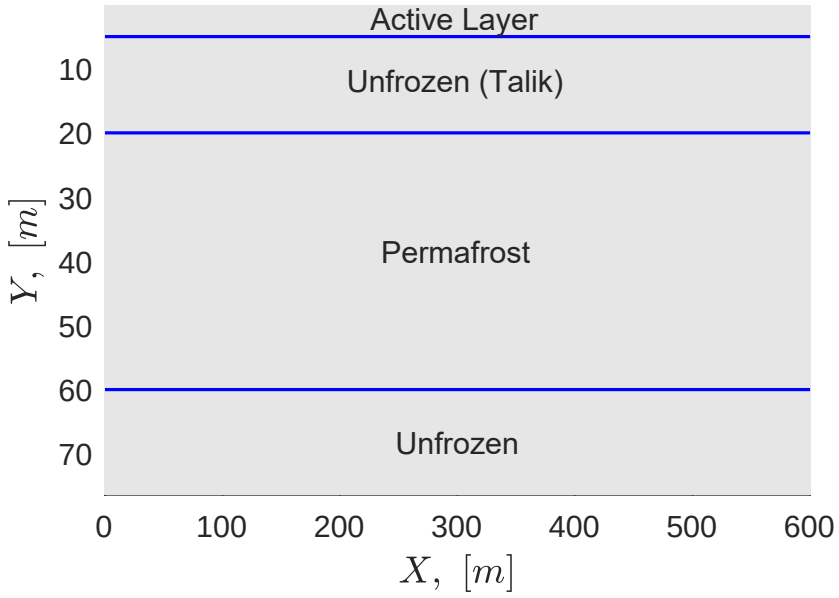

Figure 8. Description of a layered permafrost model with a talik zone.

Test 4. Let us now analyze the influence of the relaxation time on the wave field generation. Consider the same model as in the previous Test 3, fix the interphase friction $\theta_2 = 3.36 \cdot 10^{-7}$ and start to vary the values of the relaxation time τ.

By analogy with the previous figures, the horizontal through $x2 = 0$ wave field slices of the component V^2 for the porous solid+water medium with parameters from Table1, interphase friction $\theta_2 = 3.36 \cdot 10^{-7}$ and different values of the relaxation time τ are shown in Fig. 6 with the zoomed version in Fig. 7. As can be seen from the plots, the relaxation time affects both fast and slow P-wave amplitudes and shape. The smaller the τ parameter, the greater the attenuation.

Test 5. In this section, we analyze the seismic wave propagation for the permafrost model.

Based on the studies carried out in [18], we will use a typical geological profile of a permafrost area, shown in Fig. 8. The model has an upper active layer that is subject to seasonal thawing and freezing to a depth of 5 meters. From 20 to 60 meters is the permafrost zone. Between the active layer and the permafrost, at a depth of 5 to 20 meters, there is a zone of non-freezing talik. This layer usually forms when the permafrost thaws due to climate change or other factors. Below 60 meters there are bedrock formations. The seismic parameters of the model are given in Table 2.

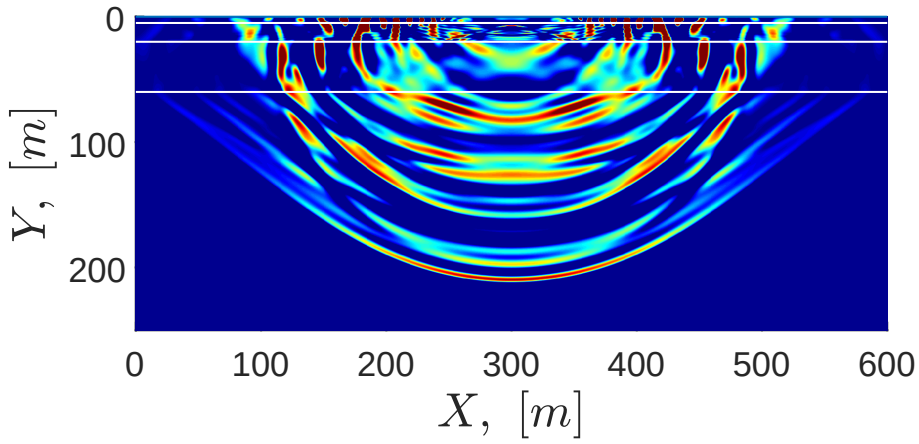

(a) Talik layer: $\alpha_1^0 = 0.001, \alpha_2^0 = 0.2, \alpha_3^0 = 0.799, \theta_1 = \theta_2 = \tau = \infty$

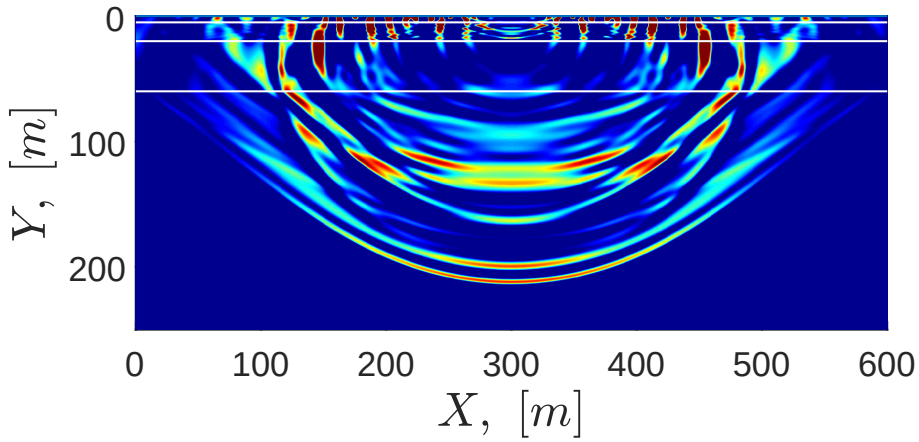

(b) Talik layer: $\alpha_1^0 = 0.001, \alpha_2^0 = 0.2, \alpha_3^0 = 0.799, \theta_1 = 3.36 \cdot 10^{-12}, \theta_2 = 3.36 \cdot 10^{-7}, \tau = 10^{-6}$

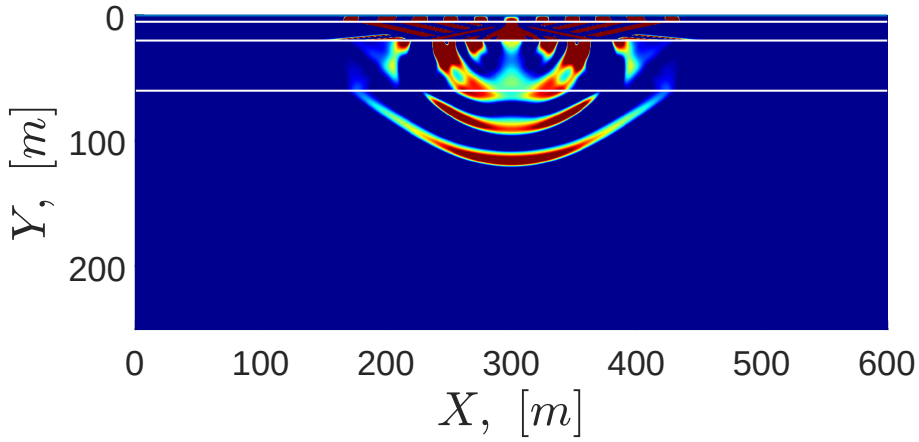

(c) Talik layer: $\alpha_1^0 = 0.1, \alpha_2^0 = 0.2, \alpha_3^0 = 0.7, \theta_1 = 3.36 \cdot 10^{-12}, \theta_2 = 3.36 \cdot 10^{-7}, \tau = 10^{-6}$

Figure 9. Snapshots of the wave field component V^2 for model with talik layer at time $t = 0.1\ s$.

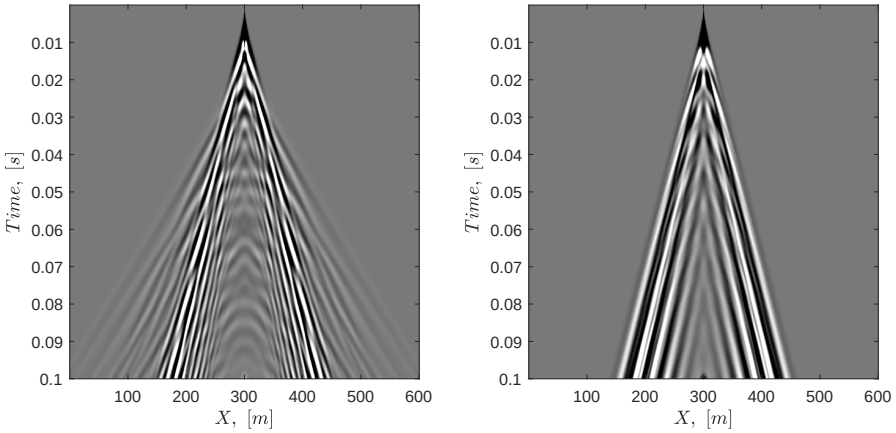

Figure 10. Seismograms of the V^2 velocity recorded in receivers on the free surface with a step 0.2m for two models with Talik layer:
(a) $\alpha_1^0 = 0.001, \alpha_2^0 = 0.2, \alpha_3^0 = 0.799, \theta_1 = \theta_2 = \infty, \tau = \infty$;
(b) $\alpha_1^0 = 0.1, \alpha_2^0 = 0.2, \alpha_3^0 = 0.7, \theta_1 = 3.36 \cdot 10^{-12}, \theta_2 = 3.36 \cdot 10^{-7}, \tau = 10^{-6}$.

Several numerical experiments have been carried out assuming that the phase ratio in the talik zone varies as well as the magnitude of the interfacial friction and the relaxation time. We assume that during heating or freezing, the proportion of air and liquid phases in this layer can change, leading to a change in the phase ratio in the mathematical model. The aim of these experiments was to demonstrate the significant influence of the phase ratio in poroelastic media on the behavior of the seismic wave field.

Simulations were performed for a computational model of $3000 * 1250$ grid nodes with a uniform spatial grid cell of 0.2 m and a time step of $2.5 \cdot 10^{-5}$ s up to time $t = 0.1$ s. The vertical source with frequency $f_0 = 150$ Hz was located on a free surface in the center.

Fig. 9 shows snapshots of the wave field component V^2 for the model with talik layer at time $t = 0.1$ s. We consider three variants of talik layer content:

- $\alpha_1^0 = 0.001, \alpha_2^0 = 0.2, \alpha_3^0 = 0.799, \theta_1 = \theta_2 = \infty, \tau = \infty$;
- $\alpha_1^0 = 0.001, \alpha_2^0 = 0.2, \alpha_3^0 = 0.799, \theta_1 = 3.36 \cdot 10^{-12}, \theta_2 = 3.36 \cdot 10^{-7}, \tau = 10^{-6}$;
- $\alpha_1^0 = 0.1, \alpha_2^0 = 0.2, \alpha_3^0 = 0.7, \theta_1 = 3.36 \cdot 10^{-12}, \theta_2 = 3.36 \cdot 10^{-7}, \tau = 10^{-6}$.

We see that adding dissipative mechanisms and increasing the air content in the talik formation leads to a change in the wave field behavior. As the

air content of the layer increases, this change becomes significant. This fact is confirmed by comparing seismogram of the V^2 velocity recorded in free surface receivers with 0.2 m spacing for two cases in Fig. 10.

5 Conclusion

The behavior of wave fields under temperature variations in a porous medium saturated with a mixture of liquid and gas was studied. The mathematical model is based on Hyperbolic Thermodynamically Compatible (HTC) systems theory, and its governing equations are applicable for the description of a compressible two-fluid mixture flow in a deformed porous medium. A linearized version of the equations for small amplitude wave propagation is derived and used for numerical modeling of seismic wave fields in poroelastic media.

In order to verify the obtained system of equations, a series of numerical tests were carried out. It has been shown that the proposed model works even in limiting cases when the volume fraction of some phases becomes 1, i.e. when the porous medium becomes pure elastic. The results obtained are consistent with the general theory of porous media and, as in the Biot model, the appearance of slow P-waves is observed. The calculated values of the wave velocities agree with the theoretical ones with an accuracy up to the error of the finite difference scheme.

The next step in the verification of the mathematical HTC model was to investigate the mechanisms of seismic wave attenuation included in the system of equations. It should be noted that the main causes of seismic energy absorption in poroelastic media are internal interfacial friction and stress relaxation, which in turn depend on pressure, temperature changes and, consequently, changes in the phase composition of the porous medium. Numerical experiments have shown that interfacial friction mainly affects the attenuation of the slow Biot P-wave, while the term responsible for shear stress relaxation affects the attenuation of the amplitudes of the fast and slow P-waves. Note that in the seismic frequency range, the slow P-wave attenuates very quickly and is not taken into account when interpreting seismic data.

We have also used the HTC model to simulate seismic wave propagation for a permafrost model with a talik and active layers. By varying the gas and liquid phase content and the relaxation mechanisms in the talik layer, we have shown their significant influence on seismic waves and the need for more specific models to simulate seismic waves in thawing zones.

Appendix

In Appendix a numerical scheme obtained by the staggered-grid finite difference approach for the approximation of the system (25) is presented. The derivation of the scheme is done by analogy with [10], [16].

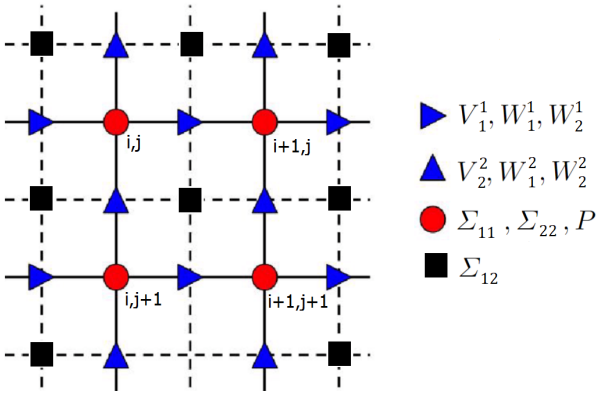

Figure 11. The relative position of deviatoric stresses, pressure, mixture velocities and relative velocities on the staggered grid.

First, within the (t, x_1, x_2) time-space framework, we construct a grid with integer nodes at $t^n = n\Delta t$, $x_1^i = i\Delta x_1$, $x_2^j = j\Delta x_2$ and semi-integer nodes at $t^{n+1/2} = (n+1/2)\Delta t$, $x_1^{i+1/2} = (i+1/2)\Delta x_1$, $x_2^{j+1/2} = (j+1/2)\Delta x_2$, where Δt, Δx_1, Δx_2 represent the grid spacings in time and space.

The staggered-grid finite difference method is based on the finite volume discretization method presented in particular in [19], and is often applied to systems of equations derived from physical conservation laws. A key advantage of this approach is that it eliminates the need to approximate fluxes during the solution as the flux values are known, increasing the efficiency and reliability of the method. As part of this technique, we define the stresses and velocities at different grid points in space and time to provide a fourth-order accuracy approximation with a minimal difference scheme template.

The material parameters are assumed to remain constant within each grid cell $[x_1^{i-1/2}, x_1^{i+1/2}] \times [x_2^{j-1/2}, x_2^{j+1/2}]$, allowing potential discontinuities along the grid boundaries.

The mixture velocity V^1 and the relative velocities W_1^1, W_2^1 are defined in nodes $(n, i+1/2, j)$ and are denoted $(V^1)^n_{i+1/2,j}, (W_1^1)^n_{i+1/2,j}, (W_2^1)^n_{i+1/2,j}$. Similarly, the components V^2, W_1^2, W_2^2 are defined at the nodes $(n, i, j+1/2)$ and are denoted as $(V^2)^n_{i,j+1/2}$ and $(W_1^2)^n_{i,j+1/2}, (W_2^2)^n_{i,j+1/2}$.

The pressure and deviatoric stresses are assigned to the integer nodes in space and semi-integer nodes in time $(n+1/2, i, j)$ as $(P)^{n+1/2}_{i,j}$, $(\Sigma_{11})^{n+1/2}_{i,j}$, $(\Sigma_{22})^{n+1/2}_{i,j}$, and the shear stress is assigned to the nodes $(n+1/2, i+1/2, j+1/2)$ and is denoted as $(\Sigma_{12})^{n+1/2}_{i+1/2,j+1/2}$. The spatial arrangement of the nodes on the staggered grid is shown in Fig.11.

For compactness, let us introduce a few notations for a discrete function $f^n_{i,j} = f(t^n, x^i_1, x^j_2)$:

- Second-order central difference operators

$$D_t[f]^n_{i,j} = \frac{(f)^{n+1/2}_{i,j} - (f)^{n-1/2}_{i,j}}{\Delta t}, \qquad A_t[f]^n_{i,j} = \frac{(f)^{n+1/2}_{i,j} + (f)^{n-1/2}_{i,j}}{2}, \quad (35)$$

- Fourth-order central difference operators (Levander stencil)

$$D_1[f]^n_{i,j} = \frac{1}{\Delta x_1}\left\{\frac{9}{8}\left((f)^n_{i+1/2,j} - (f)^n_{i-1/2,j}\right) - \frac{1}{24}\left((f)^n_{i+3/2,j} - (f)^n_{i-3/2,j}\right)\right\}, \quad (36)$$

$$D_2[f]^n_{i,j} = \frac{1}{\Delta x_2}\left\{\frac{9}{8}\left((f)^n_{i,j+1/2} - (f)^n_{i,j-1/2}\right) - \frac{1}{24}\left((f)^n_{i,j+3/2} - (f)^n_{i,j-3/2}\right)\right\}, \quad (37)$$

- Volumetric arithmetic averaging

$$\langle f\rangle^n_{i+1/2,j} = (f^n_{i,j} + f^n_{i+1,j})/2, \qquad \langle f\rangle^n_{i,j+1/2} = (f^n_{i,j} + f^n_{i,j+1})/2, \quad (38)$$

- Harmonic averaging by [20]

$$\{f\}^n_{i+1/2,j+1/2} = \left[\frac{1}{4}\left(\frac{1}{f^n_{i,j}} + \frac{1}{f^n_{i+1,j}} + \frac{1}{f^n_{i,j+1}} + \frac{1}{f^n_{i+1,j+1}}\right)\right]^{-1}. \quad (39)$$

Using these notation, the finite difference equations can be written as

$$D_t[V^1]^{n-1/2}_{i+1/2,j} = -\left\langle 1/\rho^0 \right\rangle_{i+1/2,j} D_1[P]^{n-1/2}_{i+1/2,j} + \\ + \left\langle 1/\rho^0 \right\rangle_{i+1/2,j} \left(D_1[\Sigma_{11}]^{n-1/2}_{i+1/2,j} + D_2[\Sigma_{12}]^{n-1/2}_{i+1/2,j} \right) + (\Phi^1)^{n-1/2}_{i+1/2,j},$$

$$D_t[V^2]^{n-1/2}_{i,j+1/2} = -\left\langle 1/\rho^0 \right\rangle_{i,j+1/2} D_2[P]^{n-1/2}_{i,j+1/2} + \\ + \left\langle 1/\rho^0 \right\rangle_{i,j+1/2} \left(D_1[\Sigma_{12}]^{n-1/2}_{i,j+1/2} + D_2[\Sigma_{22}]^{n-1/2}_{i,j+1/2} \right) + (\Phi^2)^{n-1/2}_{i,j+1/2},$$

$$D_t[W_1^1]^{n-1/2}_{i+1/2,j} = -\left\langle 1/\rho_1^0 - 1/\rho_3^0 \right\rangle_{i+1/2,j} D_1[P]^{n-1/2}_{i+1/2,j} - A_t[\Lambda_1^1]^{n-1/2}_{i+1/2,j},$$

$$D_t[W_2^1]^{n-1/2}_{i+1/2,j} = -\left\langle 1/\rho_2^0 - 1/\rho_3^0 \right\rangle_{i+1/2,j} D_1[P]^{n-1/2}_{i+1/2,j} - A_t[\Lambda_2^1]^{n-1/2}_{i+1/2,j},$$

$$D_t[W_1^2]^{n-1/2}_{i,j+1/2} = -\left\langle 1/\rho_1^0 - 1/\rho_3^0 \right\rangle_{i,j+1/2} D_2[P]^{n-1/2}_{i,j+1/2} - A_t[\Lambda_1^2]^{n-1/2}_{i,j+1/2},$$

$$D_t[W_2^2]^{n-1/2}_{i,j+1/2} = -\left\langle 1/\rho_2^0 - 1/\rho_3^0 \right\rangle_{i,j+1/2} D_2[P]^{n-1/2}_{i,j+1/2} - A_t[\Lambda_2^2]^{n-1/2}_{i,j+1/2},$$

$$D_t[P]^n_{i,j} = -(K)_{i,j} \left(D_1[V^1]^n_{i,j} + D_2[V^2]^n_{i,j} \right) - \\ -(K'_1)_{i,j} \left(D_1[W_1^1]^n_{i,j} + D_2[W_1^2]^n_{i,j} \right) - (K'_2)_{i,j} \left(D_1[W_2^1]^n_{i,j} + D_2[W_2^2]^n_{i,j} \right),$$

$$D_t[\Sigma_{11}]^n_{i,j} = (\mu)_{i,j} \left(\tfrac{4}{3} D_1[V^1]^n_{i,j} - \tfrac{2}{3} D_2[V^2]^n_{i,j} \right) - (1/\tau)_{i,j} A_t[\Sigma_{11}]^n_{i,j},$$

$$D_t[\Sigma_{22}]^n_{i,j} = (\mu)_{i,j} \left(\tfrac{4}{3} D_2[V^2]^n_{i,j} - \tfrac{2}{3} D_1[V^1]^n_{i,j} \right) - (1/\tau)_{i,j} A_t[\Sigma_{22}]^n_{i,j},$$

$$D_t[\Sigma_{12}]^n_{i+1/2,j+1/2} = \{\mu\}_{i+1/2,j+1/2} \left(D_1[V^2]^n_{i+1/2,j+1/2} + D_2[V^1]^n_{i+1/2,j+1/2} \right) - \\ - \{1/\tau\}_{i+1/2,j+1/2} A_t[\Sigma_{12}]^n_{i+1/2,j+1/2}.$$

The scheme obtained is an explicit finite difference scheme of forth-order accuracy in time and space for a homogeneous elastic medium. The stability conditions and dispersion properties can be found in [15].

References

[1] M.A. Biot, *Theory of propagation of elastic waves in a fluid-saturated porous solid. I. Low-frequency range*, J. Acoust. Soc. Amer., **28**:2, (1956), 168–178. MR0134056

[2] M.A. Biot, *Theory of propagation of elastic waves in a fluid-saturated porous solid. II. Higher frequency range*, J. Acoust. Soc. Amer., **28**:2, (1956), 179–191. MR0134057

[3] J.M. Carcione, C. Morency, V. Santos, *Computational poroelasticity – A review*, Geophysics, **75**:5 (2010), 75A229–75A243.

[4] F. Pesavento, B.A. Schrefler, G. Sciumè, *Multiphase flow in deforming porous media: a review*, Arch. Comput. Methods Eng., **24**:2 (2017), 423–448. Zbl 1364.76224

[5] Zhiqi Shi, Xiao He, Dehua Chen, Xiuming Wang, *Seismic wave dispersion and attenuation resulting from multiscale wave-induced fluid flow in partially saturated porous media*, Geophys. J. Intern., **236**:2 (2024), 1172–1182.
[6] S.K. Godunov, E.I. Romenskii, *Elements of continuum mechanics and conservation laws*, Kluwer, New York, 2003. Zbl 1031.74004
[7] E. Romenski, *Hyperbolic systems of thermodynamically compatible conservation laws in continuum mechanics*, Math. Comput. Modelling, **28**:10 (1998), 115—130. MR1662561
[8] I. Peshkov, M. Pavelka, E. Romenski, M. Grmela, *Continuum mechanics and thermodynamics in the Hamilton and the Godunov-type formulations*, Contin. Mech. Thermodyn., **30**:6 (2018), 1343–1378. Zbl 1439.70036
[9] E. Romenski, G. Reshetova, I. Peshkov, M. Dumbser, *Modeling wavefields in saturated elastic porous media based on thermodynamically compatible system theory for two-phase solid-fluid mixtures*, Comput. Fluids, **206** (2020), Article ID 104587. Zbl 1519.76219
[10] G. Reshetova, E. Romenski, *Diffuse interface approach to modeling wavefields in a saturated porous medium*, Appl. Math. Comput., **398** (2021), Article ID 125978.
[11] E. Romenski, G. Reshetova, I. Peshkov, *Two-phase hyperbolic model for porous media saturated with a viscous fluid and its application to wavefield simulation*, Appl. Math. Modelling, **106** (2022), 567–600. Zbl 1503.76099
[12] E. Romenski, G. Reshetova, I. Peshkov, *Computational model for compressible two-phase flow in a deformed porous medium*, In Gervasi, O., et al., *Computational Science and Its Applications – ICCSA 2021. ICCSA 2021*, Lecture Notes Computer Science, **12949**, Springer, Cham, 2021.
[13] E. Romenski, G. Reshetova, I. Peshkov, *Thermodynamically compatible hyperbolic model of a compressible multiphase flow in a deformable porous medium and its application to wavefields modeling*, AIP Conf. Proc., **2448**:1, (2021), Article ID 020019.
[14] E. Romenski, A. Belozerov, I. Peshkov, *Conservative formulation for compressible multiphase flows*, Q. Appl. Math., **74**:1 (2016), 113–136. Zbl 1336.35305
[15] J. Virieux, *P-SV wave propagation in heterogeneous media: Velocity-stress finite-difference method*, Geophysics, **51**:4 (1986), 889–901.
[16] A.R. Levander, *Fourth-order finite-difference P-SV seismograms*, Geophysics, **53**:11 (1988), 1379–1492.
[17] R.W. Graves *Simulating seismic wave propagation in 3D elastic media using staggered-grid finite differences*, Bull. Seismolog. Soc. America, **86**:4 (1996), 1091–1106.
[18] T.N. Davis, *Permafrost: a guide to frozen ground in transition*, University of Alaska Press, Fairbanks, 2001.
[19] A.A. Samarskii *The theory of difference schemes*, Marcel Dekker, New York, 2001. Zbl 0971.65076
[20] P. Moczo, J. Kristek, V. Vavrycuk, R. J. Archuleta, L. Halada, *3D heterogeneous staggered-grid finite-difference modeling of seismic motion with volume harmonic and arithmetic averaging of elastic moduli and densities*, Bull. Seismolog. Soc. America, **92**:8 (2002), 3042–3066.

Galina Vitalievna Reshetova
Institute of Computational Mathematics and Mathematical Geophysics SB RAS,
Ac. Lavrentieva ave., 6,
630090, Novosibirsk, Russia
Email address: kgv@nmsf.sscc.ru

Evgeny Igorevich Romenski
Sobolev Institute of Mathematics SB RAS,
Ac. Koptyug ave., 4,
630090, Novosibirsk, Russia
Email address: evrom@math.sscc.ru